Breakage functions of particles of four different materials subjected to uniaxial compression

The 8th International Conference for Conveying and Handling of Particulate Solids
Tel-Aviv, Israel, May 2015

BREAKAGE FUNCTIONS OF PARTICLES OF FOUR DIFFERENT MATERIALS SUBJECTED TO UNIAXIAL COMPRESSION

Dharminder Singh[1], Don McGlinchey[1] and Martin Crapper[2]
1. School of Engineering and Built Environment
Glasgow Caledonian University
Glasgow G51 1SG, United Kingdom
2. School of Engineering
The University of Edinburgh
Edinburgh EH9 3JL, United Kingdom

Abstract - Particle breakage is a common problem in the conveying and handling of particulate solids. The phenomenon of particle breakage has been studied by experiments by a number of researchers in order to describe the process of breakage by mathematical functions. The development of comminution functions that can suitably describe the breakage behaviour of granular materials can lead to a significant improvement in the design and efficiency of particulate solids handling equipment. The present study focuses on developing the strength distribution and the breakage functions of particles of four different materials subjected to uniaxial compressive loading. The determination of particle strength is an important aspect in studying particle breakage as it determines whether a particle will break under an applied force. Single particles were compressed until fracture in order to determine their strength. The strength of the particles is expressed in terms of force in this study as it can be directly obtained from the experiments. Using the crushing force data from the experiments, strength distributions of the particles were plotted and described by a statistical function. Tests were also conducted to investigate the size distribution of the fragments formed after breakage. The sizes of the fragments were measured using optical microscopy. Based on the size distribution of the fragments, breakage functions were developed for the materials.

1. INTRODUCTION

In the recent years, research on particle breakage has attracted a lot of interest in the particulate solids handling industry, where it is a common issue. Particle breakage can be desirable or undesirable depending upon the application, i.e., it is desirable in rock crushing/milling applications whereas it is undesirable in the chemical and pharmaceutical industries. In both cases, it is essential to study the process of particle breakage in order to improve the efficiency of particulate solids handling equipment.

A number of researchers have investigated the phenomenon of particle breakage by using mathematical comminution functions. Some researchers have used compression tests [1-3] whereas others have used impact tests [4, 5] to determine these comminution functions. Kalman et al. [6] presented a new method to implement five comminution functions into Discrete Element Method (DEM) simulations to simulate the process of particle breakage. These functions include strength distribution, selection, breakage, equivalence and fatigue functions. The present study focuses on determining the strength distribution and breakage functions of four different materials by using uniaxial compression tests. These functions are important because the strength distribution function determines whether a particle will break under an applied force whilst the breakage function determines the size distribution of the fragments produced as a result of particle breakage.

In the compression tests, a single particle is subjected to uniaxial compression between two platens until fracture, and the force required to break the particle is recorded as the crushing force. Due to the presence of pores and existing cracks, the strength of the particles is not uniform [1], so a large number of particles need to be tested in order to determine a statistically reliable strength distribution which can be described by a statistical function. Table 1 shows the sample sizes and the statistical functions used by some previous researchers. In this table, *P* is the probability of particle breakage, *F* is the crushing force and *a* and *b* are empirical model parameters. The logistic function has been chosen to describe the strength distribution in this study.

Table 1: Sample sizes and statistical functions used by some previous researchers

Reference	Sample size	Statistical function	Model	
Suber-Couroyer et al. [1]	200	Weibull	$P = 1 - \exp\left[-\left(\frac{F}{a}\right)^b\right]$	(1)
Aman et al. [7]	100	Lognormal	$P = \frac{1}{2}\left[1 + erf\left(\frac{\ln(F) - a}{b\sqrt{2}}\right)\right]$	(2)
Petukhov and Kalman [8]	100	Logistic	$P = 1 - \frac{1}{1 + \left(F/a\right)^b}$	(3)

According to Kalman et al. [6], the cumulative mass or volumetric breakage function B can be expressed by:

$$B = \left(\frac{d_f}{d_{max}}\right)^c \tag{4}$$

where, d_f is the fragment size, d_{max} is the largest particle size in the population of fragments and c is an empirical parameter.

In this study, the logistic function and the breakage function were applied to describe the particle strength distribution and fragment size distribution respectively, and the empirical parameters were determined.

2. EXPERIMENTS

In order to investigate particle breakage, experiments were conducted using a TA XTPlus Texture Analyser (Stable Micro Systems Ltd, Godalming, UK) which is shown in Fig. 1. It is capable of measuring physical characteristics of materials such as breakage strength, hardness, cohesion, adhesion, stiffness, etc. by compression, tension, bending or shearing tests. It is equipped with a load cell capable of measuring loads up to 30 kg (294.3 N) with a resolution of 0.1 g. The Texture Analyser is connected to a computer system which is used to control it and to record the force, displacement and time with the help of Texture Component 32 software. A cylindrical probe of 6 mm diameter was used to compress each particle at a constant rate of 1 mm/s. As the probe moves downwards, the software records the force and displacement values, and generates a graph which can be used to determine the breakage force. When the maximum value of the force is reached and the particle cannot be compressed further, the probe retracts to its original position.

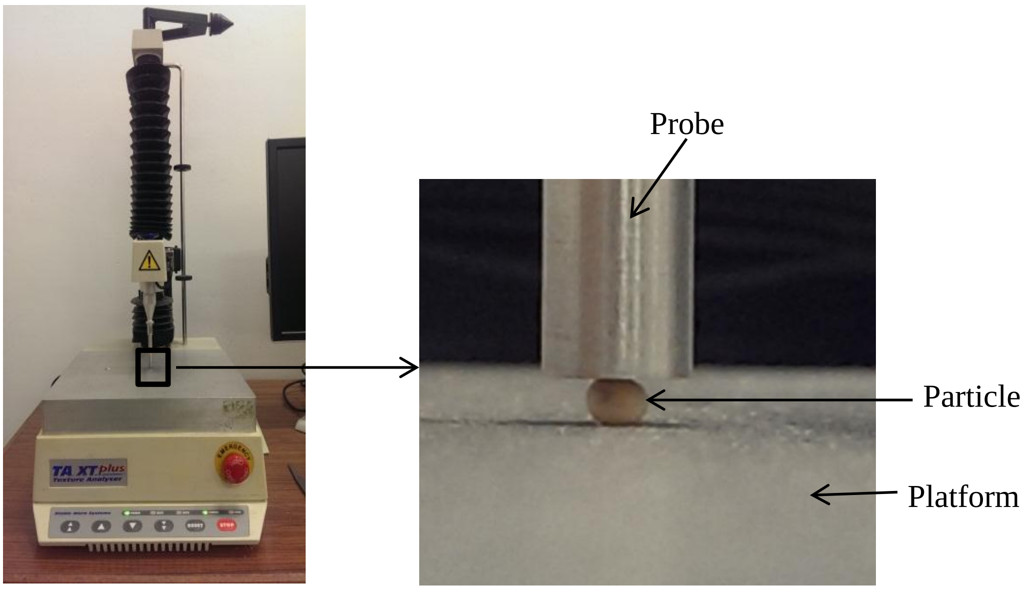

Fig. 1: TA XTPlus Texture Analyser

The first set of experiments for finding the strength distribution function were conducted using 100 particles each of four different materials. The particle size was measured with a Vernier calliper before testing each particle. Then the particle was placed on the platform and Texture Component 32 software was used to start the compression test. Table 2 lists the materials used and their sizes, whilst Fig. 2 illustrates the particles used. All the particles tested were nominally spherical apart from the unrefined cane sugar particles. It was found the mustard particles do not break into fragments, but are simply compressed.

A second set of experiments was conducted to study the size distribution of the fragments resulting from particle breakage. These involved testing 10 particles of each material except the mustard seeds, which did not break. For these experiments, each test was stopped after the particle broke. The fragments formed were then carefully collected on glass slides, to be examined by optical microscopy using a Leica DM500 microscope.

Table 2: Materials

Material	Size (mm)
Mustard Seeds	1.6-2.6
Black peppercorns	3.4-5.4
Unrefined cane sugar	0.8-2.2
Cake decorations	1.2-2.0

(a)

(b)

(c)

(d)

Fig. 2: (a) Mustard seeds (b) Peppercorns (c) Unrefined cane sugar (d) Cake decorations

3. RESULTS AND DISCUSSION

A typical force-displacement curve obtained for a black peppercorn particle of size 4.14 mm is shown in Fig. 3. The graph has been divided into four regions. In Region A, the probe is moving towards the particle so the force is zero. When the probe comes in contact with the particle at the start of Region B, the force starts to rise as the particle is being compressed. The force continues to rise until the particle breaks at which point the force drops suddenly. The probe continues to compress the fragments of the particle which are further broken into smaller fragments which appear as peaks in Region C. When the fragments are completely compressed, the force begins to rise at a higher rate as can be seen in Region D after which the probe returns to its original position and it is ready to test the next particle.

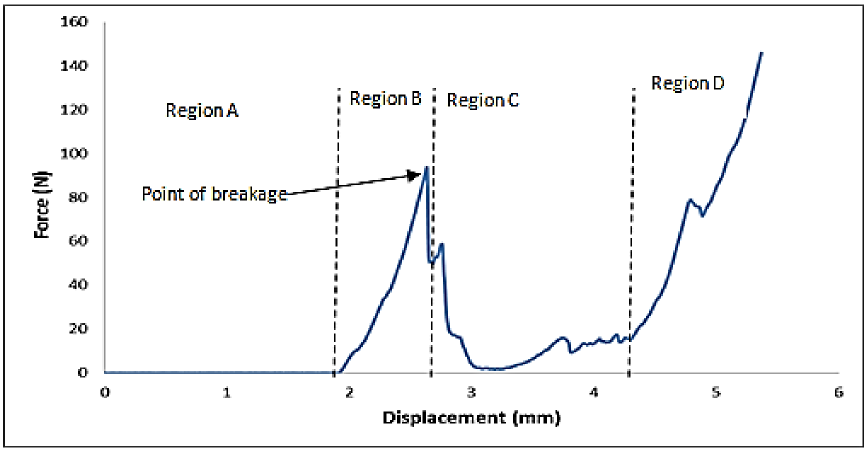

Fig. 3: Typical force vs displacement curve for a 4.14 mm peppercorn particle

3.1 Strength Distribution Function

The strength of the particles is expressed in terms of crushing force in this study which was obtained from the peak in the Region B of Fig. 3. The crushing force was recorded for all the particles and the results are shown in Table 3. The table shows the maximum, minimum, mean, median and standard deviation of crushing force found for material. As mentioned earlier, it can be seen that there is wide variation in the strength for each of the materials.

Table 3: Summary of crushing force results

Force (N)	Mustard Seeds	Peppercorns	Unrefined cane sugar	Cake decorations
Maximum	36.11	123.56	57.25	40.82
Minimum	5.91	12.31	1.13	5.23
Mean	21.68	61.10	15.16	22.45
Median	20.83	56.45	14.09	22.29
Standard deviation	4.47	26.36	9.11	6.73

As mentioned before, in order to describe the particle strength distribution, a statistical function is needed. Rozenblat et al. [3] reported that all the functions mentioned in Table 1 can describe the strength distribution satisfactorily but they chose the logistic function (Eq. (3)) for its mathematical simplicity. It does not consist of any complex mathematical expressions such as an exponent function (in Weibull) or an error function (in lognormal). For the same reason, the logistic model was chosen to represent the strength distribution of the particles in this study. The parameters also have statistical meanings: parameter a is the median, and parameter b is the dispersion of the distribution. If b is larger, the distribution would be smaller and if it is smaller, the distribution would be wider.

The logistic function was then fitted to the experimental data using the Least Mean Squares method. The values of parameters a and b and coefficient of determination R^2 were determined and are shown in Table 4. It can be seen that the values of parameter a are quite close to the median crushing force values determined from the experiments. Fig. 4 shows the logistic function fit for all the materials, from which it is clear that the logistic function describes the experimental data well.

Table 4: Logistic function fitting summary

	Mustard Seeds	Peppercorns	Unrefined cane sugar	Cake decorations
a	21.19	56.44	13.42	21.77
b	8.99	3.57	2.75	5.71
R^2	0.9919	0.9962	0.9904	0.9971

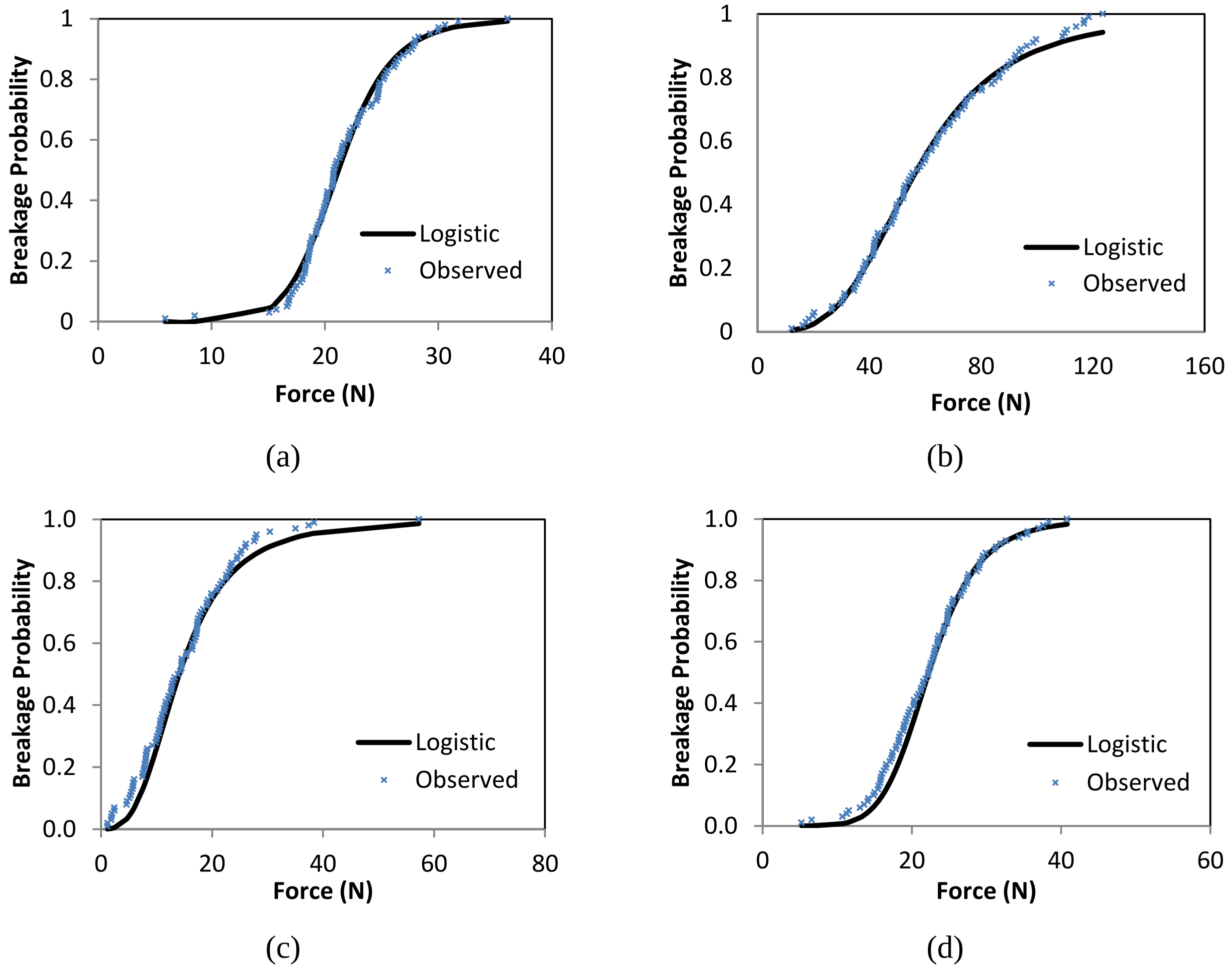

Fig. 4: Logistic function fit: (a) mustard seeds (b) peppercorns (c) unrefined cane sugar (d) cake decorations

3.2 Breakage function

This section describes the size distributions of fragments formed from the particles and how the breakage functions were determined. It was found that peppercorn particles typically break into 3 to 5 fragments. Cake decorations were found to break into 8 to 111 fragments and unrefined cane sugar into 21 to 65 fragments out of which 3 to 10 fragments accounted for 90% of the mass of the parent particle, the remaining fragments being very small.

The mass of a fragment relative to the parent particle can be determined using the following relation:

$$m_{rel} = \frac{m_f}{m_T} \quad (5)$$

where, m_f is the mass of the fragment and m_T is the total mass of the fragments, which is also equal to the mass of the parent particle.

The breakage functions determined in this study will be used in a DEM code in which spherical fragments are created after breakage [9]. Thus, for a fragment of size d_f and the parent size d_p (assuming constant density), Eq. (5) can be written as:

$$m_{rel} = \frac{V_f \rho}{V_p \rho} = \frac{\frac{1}{6}\pi d_f^3}{\frac{1}{6}\pi d_p^3} = \left(\frac{d_f}{d_p}\right)^3 \quad (6)$$

The sum total of relative mass of all the fragments found by this method will be greater than unity. Therefore, relative mass of the fragments was normalised dividing it by the sum of the relative mass of all the fragments as shown in Eq. (7).

$$m_{norm} = \frac{m_{rel}}{\sum m_{rel}} \quad (7)$$

The fragment sizes measured by microscope were used to calculate the relative mass of fragments using Eq. 6 which was then normalised using Eq. 7. Fig. 5 shows the typical size distributions of fragments obtained using this method for a particle of each material. The horizontal axis shows the cumulative normalised mass while the vertical axis shows the cumulative ratio of number of fragments to total fragments. The peppercorn, unrefined cane sugar and cake decoration particles broke into 5, 28 and 111 fragments respectively. From the 5 fragments of the peppercorn particle shown here, 4 were found to be nearly the same size and 1 a smaller size whereas the cake decoration and the unrefined cane sugar particles produced a large variety of fragment sizes. From a total of 111 fragments of the cake decoration particle, only 6 fragments make up the 90% of the mass of the parent particle. The remaining 10 % of the mass is split into the rest of the 105 fragments. A similar pattern can be seen for the unrefined cane sugar particle where the mass of just 3 fragments (from a total of 28) is equal to 90% of the parent particle and the remaining 25 fragments form just 10% of the mass of parent particle.

The breakage function (Eq. (4)) was then fitted to the cumulative normalised mass distribution of the fragments using the Least Mean Squares method and the parameter *c* was determined. The curve fitting is shown in Fig. 6. The graphs show cumulative normalised mass on the vertical axis and the particle size on the horizontal axis. It can be seen that there is a good agreement between the breakage function and the experimental data. Table 5 shows the values of parameter c obtained from the curve fitting procedure.

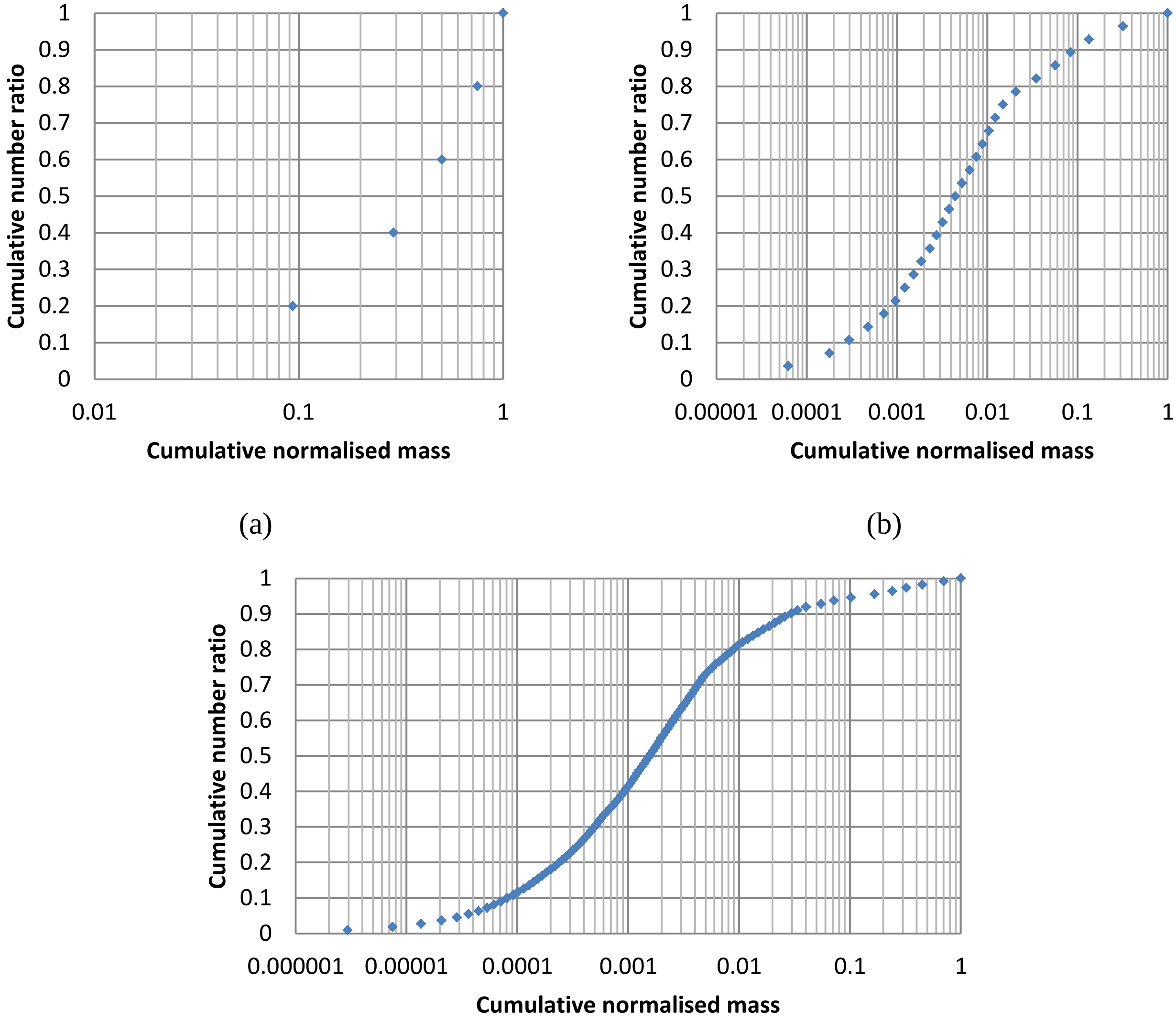

(a)

(b)

(c)

Fig. 5: Typical size distributions in terms of cumulative normalised mass (a) 4.3 mm peppercorn particle (b) 1.6 mm unrefined cane sugar particle (c) 2.02 mm cake decoration particle

Table 5: Parameter *c*

c	Peppercorns	Cake decorations	Cane sugar
Range	4.05-13.99	2.81-9.06	1.82-4.03
Mean	6.38	4.54	2.71

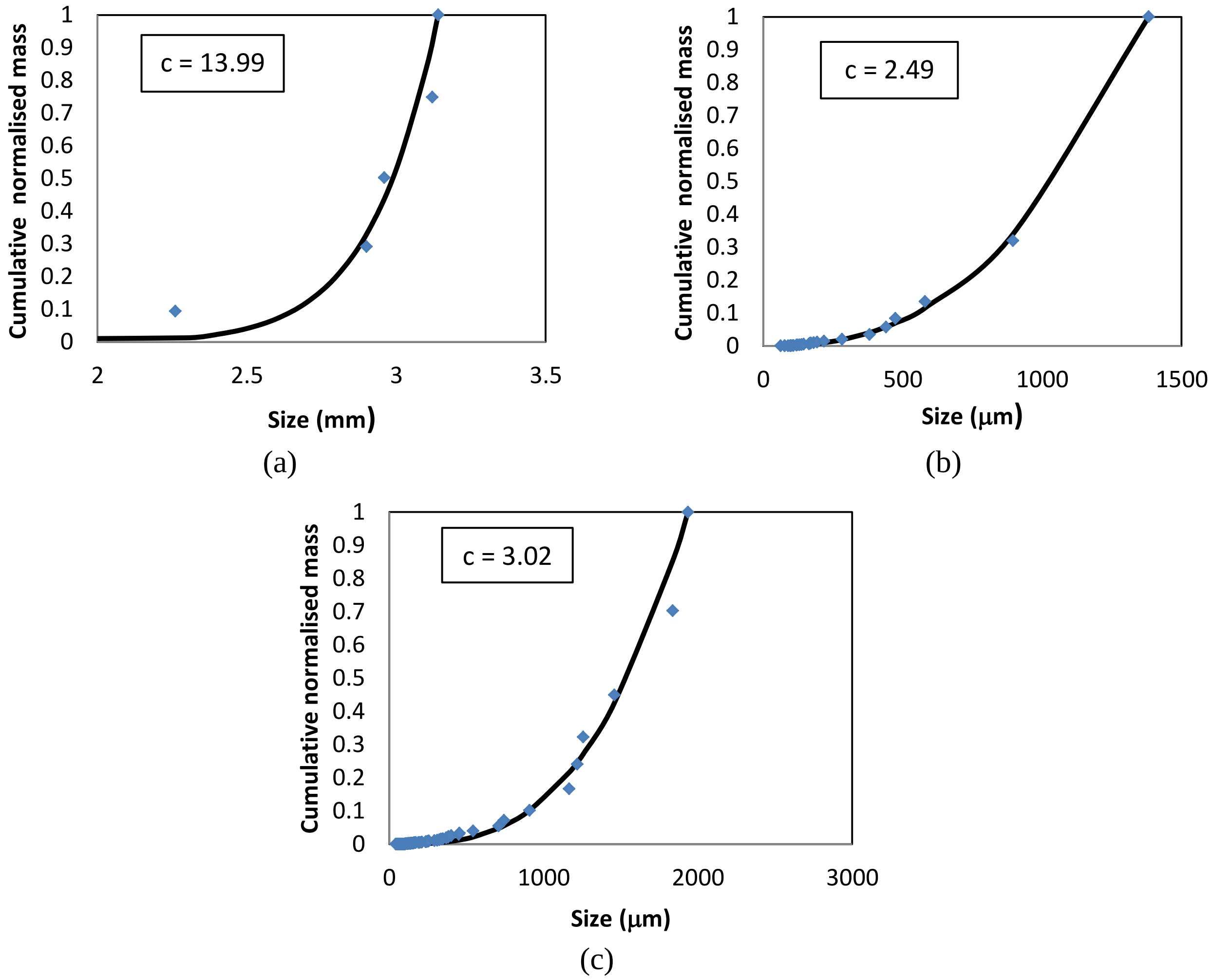

Fig. 6: Curve fitting of breakage function to normalised mass (a) 4.3 mm peppercorn particle (b) 1.6 mm unrefined cane sugar particle (c) 2.02 mm cake decoration particle. The solid line represents the breakage function and the points represent experimental data.

4. CONCLUSION

The focus of this study was to determine the strength distribution and breakage functions of mustard seeds, peppercorns, unrefined cane sugar and cake decorations by subjecting them to uniaxial compression. It was found that the mustard seeds do not fragment, while all the other materials tested do. A logistic function was fitted to the strength distribution of the materials and its empirical parameters were determined. The fragments formed from breakage of peppercorns, unrefined cane sugar and cake decoration particles were investigated to determine their breakage function. From the results, it can be concluded that the chosen mathematical functions are suitable to describe the strength distributions of the particles and the size distribution of the fragments. These functions will be used to carry out DEM simulations with these materials.

5. REFERENCES

1. C. Subero-Couroyer, M. Ghadiri, N. Brunard and F. Kolenda, "Weibull Analysis of Quasi-Static Crushing Strength of Catalyst Particles," *Chemical Engineering Research and Design,* **81**, pp. 953-962, 2003.
2. R. Pitchumani, O. Zhupanska, G. M. H. Meesters and B. Scarlett, "Measurement and characterization of particle strength using a new robotic compression tester," *Powder Technology,* **143–144**, pp. 56-64, 2004.
3. Y. Rozenblat, D. Portnikov, A. Levy, H. Kalman, S. Aman and J. Tomas, "Strength distribution of particles under compression," *Powder Technology*, **208**, pp. 215-224, 2011.
4. L. Vogel and W. Peukert, "Characterisation of Grinding-Relevant Particle Properties by Inverting a Population Balance Model," *Particle & Particle Systems Characterization,* **19**, pp. 149-157, 2002.
5. S. Z. Wu, K. T. Chau and T. X. Yu, "Crushing and fragmentation of brittle spheres under double impact test," *Powder Technology,* **143–144**, pp. 41-55, 2004.
6. H. Kalman, V. Rodnianski and M. Haim, "A new method to implement comminution functions into DEM simulation of a size reduction system due to particle-wall collisions," *Granular Matter,* **11**, pp. 253-266, 2009.
7. S. Aman, J. Tomas and H. Kalman, "Breakage probability of irregularly shaped particles," *Chemical Engineering Science,* **65**, pp. 1503-1512, 2010.
8. Y. Petukhov and H. Kalman, "Empirical breakage ratio of particles due to impact," *Powder Technology,* **143–144**, pp. 160-169, 2004.
9. T. Brosh, H. Kalman and A. Levy, "Fragments spawning and interaction models for DEM breakage simulation," *Granular Matter,* **13**, pp. 765-776, 2011

6. NOMENCLATURE

Symbol	Description	Units
a	Strength distribution function parameter	N
b	Strength distribution function parameter	-
c	Breakage function parameter	-
d_f	Size of the fragment	m
d_{max}	Size of the largest fragment	m
d_p	Size of the parent particle	m
m_f	Mass of the fragment	kg
m_{rel}	Relative mass	kg
m_{norm}	Normalised mass	kg
m_T	Total mass of fragments	kg
B	Breakage function	-
F	Force	N
P	Breakage probability	-
V_f	Volume of fragment	m^3
V_p	Volume of parent particle	m^3
ρ	Particle density	kg/m^3

7. ACKNOWLEDGEMENT

This research is part of a PhD project funded by Glasgow Caledonian University. We also acknowledge the support of Mr. Andrew Cowell in setting up the experiments.